

Fabrication of Poly (Toluidine Blue O) Functionalized Multiwalled Carbon Nanotubes on Glassy Carbon Electrode for Hydrazine Detection

Balasubramanian Sriram¹, Tse-Wei Chen², Shen-Ming Chen^{2,*}, Karuppasamy Kohilarani¹, Rajkumar Devasenathipathy¹, Sea-Fue Wang^{1,*}

¹ Department of Materials and Mineral Resources Engineering, National Taipei University of Technology, Taipei, Taiwan.

² Electroanalysis and Bioelectrochemistry Lab, Department of Chemical Engineering and Biotechnology, National Taipei University of Technology, No. 1, Section 3, Chung-Hsiao East Road, Taipei 106, Taiwan, ROC.

*E-mail: smchen78@ms15.hinet.net, sfwang@ntut.edu.tw

Received: 25 January 2018 / Accepted: 13 March 2018 / Published: 10 April 2018

Herein, we present an amperometric sensor for hydrazine developed via simple potentiodynamic electrochemical polymerization of O-Toluidine Blue (pTBO) on functionalized multi walled carbon nanotubes (*f*-MWCNTs) coated glassy carbon electrode (GCE). The obtained of *f*-MWCNTs/pTBO composite was confirmed through FESEM, EDX and cyclic voltammetric studies. Relative to pTBO modified electrodes, *f*-MWCNTs/pTBO modified GCE displayed a well-defined electro-oxidation peak current response towards the detection of hydrazine. *f*-MWCNTs/pTBO/GCE exposes its good electrocatalytic ability in a wide linear range from 1 μM to 357 μM . Our modified electrode also possesses low limits of detection (0.24 μM) with high sensitivity (2492 $\mu\text{A mM}^{-1} \text{cm}^{-2}$) value. The successful demonstration of feasible practicality of *f*-MWCNTs/pTBO composite modified GCE was performed in untreated rain, lake and tap water samples.

Keywords: Amperometric sensor, O-Toluidine Blue, Functionalized multi walled carbon nanotubes, Hydrazine.

1. INTRODUCTION

Hydrazine, an inorganic flammable liquid, has been extensively used in agriculture, pharmaceutical industry and also as a propellant in space vehicles[1, 2]. Based on the nature of toxicity, EPA (Environmental Protection Agency) and WHO (World Health Organization) have categorized hydrazine as a carcinogenic agent (group B2)[3, 4]. The harmful effects of highly toxic

hydrazine include kidney, liver and also brain damages in humans. Therefore, the determination of hydrazine is essential in both environmental and biological means. Relative to other analytical techniques such as potentiometry[5], titrimetry[6], fluorescence[7], flow-injection chemiluminescence [8], high-performance liquid chromatography[9] and Spectrophotometry[10], electrochemical methods[11] are highly preferred by the present-day researchers due to their simple protocol, low price, highly sensitive and selective nature with good repeatability and reproducibility[12]. In contrast, the unmodified (bare) electrodes employed in electrochemical methods have their own disadvantages like high over potential, electrode fouling and poor electron transfer[13, 14]. In order to overcome these drawbacks, current researchers prefer the working electrodes which are chemically modified using O-aminophenol[15], benzofuran derivatives[16], Vitamin B12[17] and Pd-TiO₂[18] *etc.*, Based on the issues, low cost and good electroactive materials are more desirable for the chemical modification of electrodes.

Recently, O-Toluidine Blue (TBO), a member of thiazine group has received more attention in developing the modified electrodes for the determination of certain compounds such as alcohol[19], glucose[20], NADH[21], and hydrogen peroxide[22]. The further enhancement of stability and electrochemical activity of TBO modified electrodes can be done by coalescing conducting polymers[23], metal[24] nanomaterials or carbon materials[21]. Among various available carbon materials (graphene, graphene oxide, carbon nanotubes, etc.), carbon nanotubes are extensively used in the field of sensing and bio-sensing research[25]. Compared to single walled carbon nanotubes (SWCNTs), multi walled carbon nanotubes (MWCNTs) are more desirable because of their high surface area, superior charge-transport property, higher chemical stability and excellent mechanical strength[26]. On the other hand, MWCNTs suffer poor aqueous dispersion due to the hydrophobic nature. In recent years, the functionalized MWCNTs (*f*-MWCNTs) resulting from the acid treatment of MWCNTs possess higher aqueous dispersion[27].

Based on the advantages of both TBO and *f*-MWCNTs, a modified glassy carbon electrode (*f*-MWCNTs/pTBO/GCE) has been fabricated for hydrazine determination. *f*-MWCNTs utilized in the construction of our hydrazine sensor have enhanced the conductance and electrocatalytic activity of pTBO. *f*-MWCNTs/pTBO modified electrode exposed an increased electrocatalytic ability towards the determination of hydrazine in terms of the electroanalytical parameters (linear range, limits of detection and sensitivity). Our fabricated electrode also showed high storage stability with good repeatability and reproducibility.

2. EXPERIMENTAL

2.1 Materials and Methods

Functionalized multi walled carbon nanotubes (*f*-MWCNTs), O-Toluidine Blue (TBO), potassium hydroxide (KOH) and hydrazine (N₂H₄) were purchased from Sigma-Aldrich at an analytical grade and used without any further purification. 0.1 M KOH was utilized as the supporting electrolyte for the entire electrochemical studies. Prior to each experiment, all the solutions were

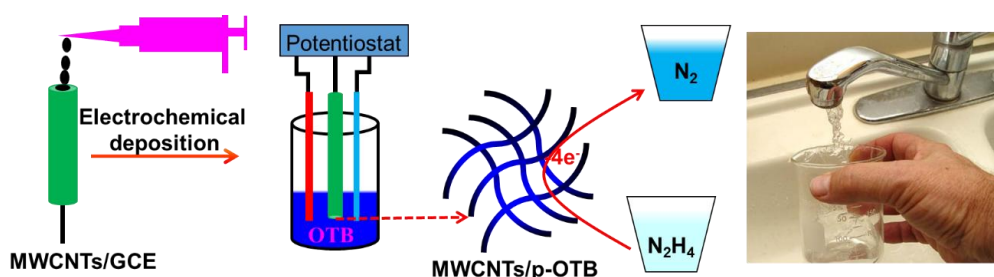
deoxygenated with pre-purified N_2 gas for 15 min unless otherwise specified. Double distilled water (conductivity $\geq 18 M\Omega\text{ cm}$) was used throughout the electrochemical experiments.

2.2 Apparatus

CHI 6171D work station in a conventional three electrode system with modified GCE (area = 0.071 cm^2) as working electrode, saturated $Ag|AgCl$ (saturated KCl) as reference electrode and Pt wire as counter electrode was utilized to perform the electrochemical experiments. Amperometric ($i-t$) studies were carried out using analytical rotator AFMSRX (PINE instruments, USA) with a rotating disc glassy carbon electrode (RDE, area 0.21 cm^2). Hitachi S4700 and HORIBA EMAX X-ACT were employed in the respective field emission scanning electron microscopy (FESEM) and energy dispersive X-ray (EDX) analysis.

2.3 Preparation of f -MWCNTs/pTBO Composite.

The surface of unmodified GCE (glassy carbon electrode) was formerly polished with a Buehler polishing kit using $0.05\text{ }\mu\text{m}$ alumina slurry, washed with water and dried at apposite conditions. $10\text{ }\mu\text{l}$ aqueous solution of f -MWCNTs (2 mg/ml) was drop cast on the previously cleaned GCE and air-dried at 40° C . In order to attain the equilibrium, f -MWCNTs/GCE was immersed in the aqueous solution of TBO for 2 min. Later, the electrochemical potentiostatic (polymerization) deposition of TBO was performed at f -MWCNTs/GCE for the potential between -0.2V – 0.6V (vs. $Ag|AgCl$). The resulting modified electrode was noted as f -MWCNTs/pTBO/GCE (**Scheme 1**). The removal of unadsorbed TBO was carried out by dipping f -MWCNTs/pTBO composite modified GCE in double distilled water and air-dried at 40° C . As control, pTBO modified GCEs was fabricated by following the same procedure.



Scheme 1. Schematic representation for the fabrication of f -MWCNTs/pTBO nanocomposite and the electrochemical performance towards oxidation of N_2H_4 .

3. RESULTS AND DISCUSSION

3.1 Characterization of f -MWCNTs/ pTBO nanocomposite

Cyclic voltammetry technique was used in the preparation of pTBO and f -MWCNTs/ pTBO. The cyclic voltammograms in **Fig. 1** show the electrochemically polymerized TBO on bare GCE (**a**)

and *f*-MWCNTs modified GCE (b). The redox current for both pTBO/GCE and *f*-MWCNTs/pTBO/GCE was increased accordingly with the increasing successive sweep between the potential of -0.2 V and 0.6 V in 0.1M H₂SO₄ at 50 mV/s scan rate. Notably, the electro polymerized TBO on *f*-MWCNTs/GCE shows several times higher peak redox current compared to electro polymerized TBO on unmodified GCE. This indicates that the hydrophilicity of MWCNTs provides large surface area for the higher deposition TBO. The adsorption strength of TBO on *f*-MWCNTs/GCE is higher compared to only unmodified GCE [21]. Thus, the redox current of *f*-MWCNTs/ pTBO/GCE is larger than that of pTBO/GCE.

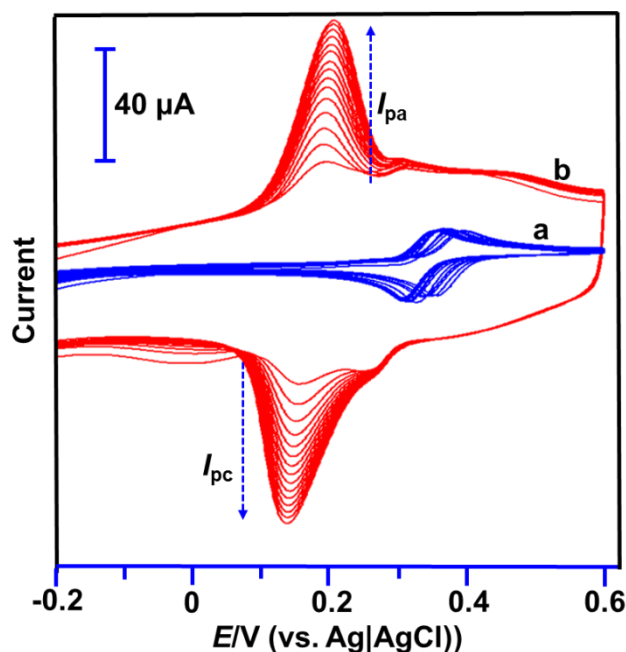


Figure 1. CVs for the electro polymerization of 1 mM toluidine blue O in 0.1 M H₂SO₄ at unmodified (bare) glassy carbon electrode (a) and *f*-MWCNTs-modified glassy carbon electrode (b). Scan rate: 50 mV/s.

Scanning electron microscopy and energy Dispersive X-ray (EDX) spectroscopy were used to study the morphology and elemental composition of the prepared nanocomposites. The SEM images of only *f*-MWCNTs and *f*-MWCNTs/pTBO were presented in Fig. 2 (A&B). The SEM image of *f*-MWCNTs/pTBO shows the highly dense pTBO covered surface compared to typical SEM image of *f*-MWCNTs. Moreover, the polymerized TBO is homogeneously adsorbed on the surface of *f*-MWCNTs. This indicates the successful formation of pTBO thin film on the surface of *f*-MWCNTs. The elements carbon, nitrogen, oxygen and sulphur with their corresponding weight percentages of 84.39, 6.87, 7.53 and 1.21 were obtained by the EDX spectrum. It can be apparently seen that the considerable weight percentages of nitrogen, oxygen and Sulphur were acquired from the formed pTBO. This EDX elemental mapping (Fig.2C) validate the successful formation of pTBO thin film on the surface of *f*-MWCNTs.

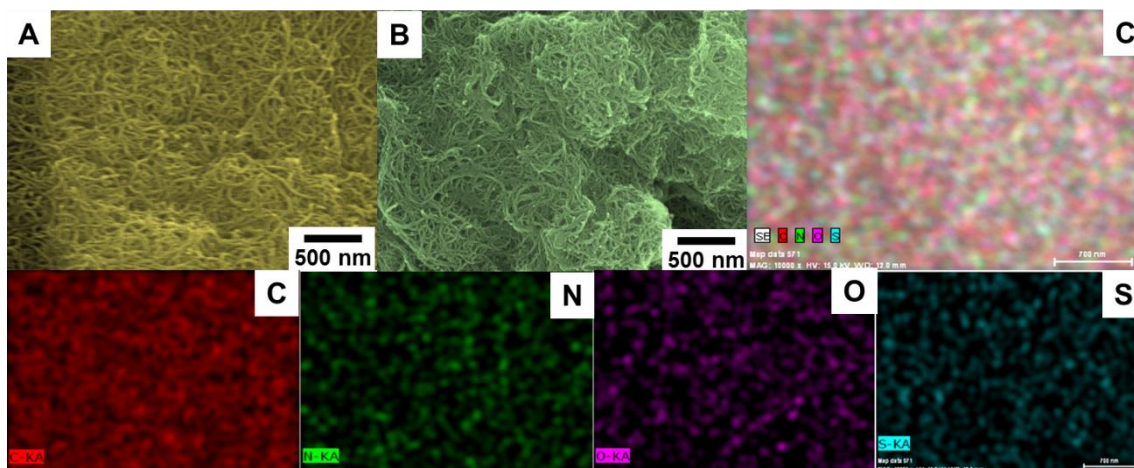


Figure 2. (A) SEM image of *f*-MWCNTs & (B) *f*-MWCNTs/ pTBO. (C) Elemental mapping of *f*-MWCNTs/ pTBO (C, N, O and S)

3.2 Electro-oxidation of hydrazine at pTBO and *f*-MWCNTs/ pTBO modified electrodes

Fig. 3 displays the CVs at *pTBO* and *f*-MWCNTs/*pTBO* modified glassy carbon electrode in 0.1 M KOH in absence (a&c) and presence (b&d) of 0.5 mM hydrazine. Because of the considerable electrocatalytic ability of *pTBO*, a broad oxidation peak response of $-74.4 \mu\text{A}$ was obtained (potential = 0.425 V) at *pTBO*/GCE towards 0.5 mM hydrazine. Relative to *pTBO*/GCE, a well-defined anodic peak response ($-443 \mu\text{A}$) with low over potential was observed at *f*-MWCNTs/*pTBO* modified GCE. The oxidation peak current response acquired at *f*-MWCNTs/*pTBO*/GCE was higher than *pTBO*/GCE (5 folds). Several functional groups present in *f*-MWCNTs enhances the high incorporation of *pTBO* and led to the excellent catalytic activity of *f*-MWCNTs/*pTBO*/GCE towards the determination of hydrazine.

3.3 Effect of concentration

The CVs for the absence (curve a) and presence (curve b-k) of hydrazine (each addition of 0.5 mM) at *f*-MWCNTs/*pTBO*/GCE in 0.1 M KOH between the applied potential of -0.2V and 0.6 V were displayed in **Fig. 4**. The scan rate was fixed at 50 mV/s. In the absence of hydrazine, no obvious anodic peak response was shown by the modified electrode. Whereas, in the presence of 0.5 mM hydrazine, a noteworthy peak current response was seen at the potential of 0.345 V. The further addition of increasing hydrazine concentration correspondingly showed an increase in the oxidation peak response. The linearity of increasing anodic peak current response (from the figure) revealed the excellent electrocatalytic activity of *f*-MWCNTs/*pTBO* modified GCE towards hydrazine.

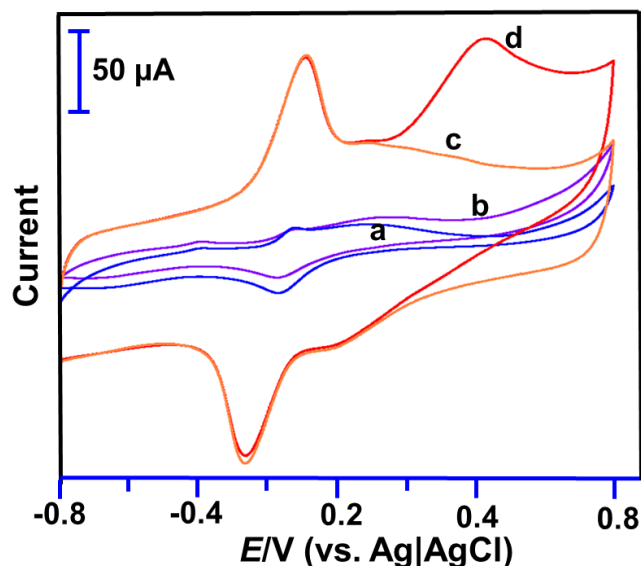


Figure 3. CVs obtained at (a) pTBO and (b) pTBO-MWCNTs film modified GCEs in 0.1 M KOH containing 1 mM hydrazine.

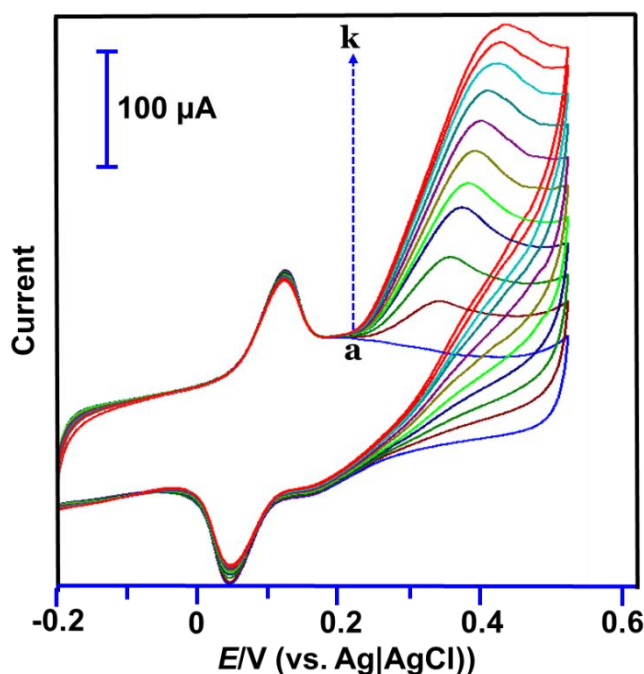


Figure 4. CVs obtained at pTBO-MWCNTs/GCE in the absence (a) and presence (b-k) of 0.5–5 mM hydrazine (each addition of 0.5 mM) in 0.1 M KOH at the scan rate 50 mV/s.

3.4 Amperometric Determination of Hydrazine

The amperogram for the detection of hydrazine at *f*-MWCNTs/pTBO modified GCE in 0.1 M KOH through amperometric *i*-*t* technique are shown in **Fig. 5**. The applied potential, scan rate and rotation speed for this study were fixed to be 0.4 V and 1500 rpm. The amperograms were recorded for the consecutive additions of varying hydrazine concentrations (1, 2, 5, 10, 30 μ M (a-e)). For each

successive addition of hydrazine, a fast and steady amperometric response was obtained at *f*-MWCNTs/pTBO modified GCE. The efficient electro-oxidation of hydrazine at the fabricated electrode was indicated by the attained steady state response current within 4 s for each addition. From the inset calibration plot, the values of linear range, limits of detection (LOD) and sensitivity were calculated to be 1–357 μM , 0.24 μM and 2492 $\mu\text{A mM}^{-1} \text{cm}^{-2}$. The equation, $\text{LOD} = 3s_b/S$ (where, s_b = standard deviation of blank signal and S = sensitivity) was used to calculate the value of sensitivity. The evaluated values of linear range, LOD and sensitivity were in concordance with the calculated electroanalytical parameters of the formerly reported hydrazine sensors in the literatures (**Table 1**). According to the Table 1, the linear range of our proposed fabricated electrode is higher, compared to Ni(II)-baicalein complex/MWCNT, Curcumin/MWCNTs and Di hydroxyl benzene salophen modified electrodes. Relative to Ag-nanozeolite, Curcumin/MWCNTs and Di hydroxyl benzene salophen based hydrazine sensors, *f*-MWCNTs/pTBO/GCE displays a low value of LOD. Also, *f*-MWCNTs/pTBO modified GCE showed a satisfying sensitivity (2492 $\mu\text{A mM}^{-1} \text{cm}^{-2}$) in the detection of hydrazine.

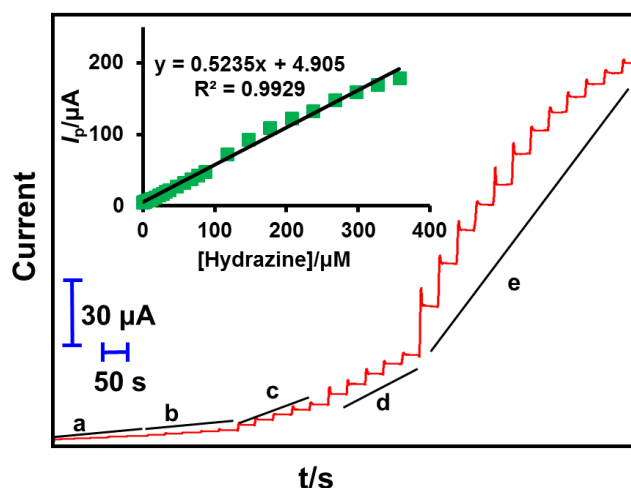


Figure 5. Amperometric *i-t* response of *f*-MWCNTs/pTBO modified rotating disc GCE upon addition of 1, 2, 5, 10, 30 μM (a-e) hydrazine in 0.1 M KOH (rotation speed = 1500 RPM, $E_{\text{app}} = + 0.30$ V). Inset: Plot of [Hydrazine] vs. I_p .

Table 1. Comparative data of *f*-MWCNTs/pTBO/GCE with other different modified electrodes towards the electro-oxidation of hydrazine

Modified Electrode	Linear range (μM)	^b LOD (μM)	Sensitivity	Ref.
Ni(II)-baicalein complex/MWCNT	2.5–200	0.8	$69.9 \mu\text{A mM}^{-1} \text{cm}^{-2}$	[28]
Ag dendrites	100-1700	0.5	$20.81 \mu\text{A mM}^{-1} \text{cm}^{-2}$	[29]
Prussian blue @AgNPs	^c NA	0.49	$26.06 \text{ A mol}^{-1} \text{ L}$	[30]
Ag-nanozeolite	12-15000	3.72	$128.7 \mu\text{A mM}^{-1} \text{cm}^{-2}$	[31]
Curcumin/MWCNTs	2–44	1.42	$22.9 \text{ nA } \mu\text{M}^{-1} \text{cm}^{-2}$	[32]
Quinizarine	0.2–1.0, 2.0–10	0.14	–	[33]
Quinizarine/TiO ₂ nanoparticles	0.5–1900	0.077	–	[34]
Di hydroxyl benzene salophen	10–400	1.6	$17 \mu\text{A mM}^{-1} \text{cm}^{-2}$	[35]

Benzofuran derivative/CNT	0.1–600	0.066	$70.1 \mu\text{A mM}^{-1} \text{cm}^{-2}$	[16]
MWCNT/B12	2–1950	0.7	$1320 \mu\text{A mM}^{-1} \text{cm}^{-2}$	[17]
Ag@Fe ₃ O ₄	0.25–3400	0.06	$270 \mu\text{A mM}^{-1} \text{cm}^{-2}$	[36]
Pd/Co-NCNTs	0.05–56.45	0.007	$343.909 \mu\text{A mM}^{-1}$	[37]
<i>f</i> -MWCNTs/pTBO/GCE	1–357	0.24	$2492 \mu\text{A mM cm}^{-2}$	This work

3.5 Selectivity studies

The selectivity examination of *f*-MWCNTs/pTBO/GCE was also carried out using amperometric *i-t* method under the same experimental conditions of section (3.4). A sharp peak current response was observed for the addition of 50 μM . In contrast, no noticeable response was obtained for the additions of 100 folds excess concentrations of other common interferents such as K⁺, Na⁺, Fe²⁺, Cu²⁺, Ca²⁺, Mg²⁺, Zn²⁺, Fe³⁺, NO₂⁻, NO₃⁻, F⁻, Cl⁻, Br⁻, I⁻, (COO)₂²⁻, fructose, glucose, and lactose. Thus, the excellent selectivity was revealed from the well-defined peak response of our sensor towards the lower hydrazine concentration (50 μM) in presence of other interferents with higher concentration.

3.6 Stability, repeatability and reproducibility studies

The storage stability of *f*-MWCNTs/pTBO modified GCE was tested by monitoring the peak current response towards 50 μM hydrazine for 30 days and stored in 0.1 M KOH at 4° C. Even after the storage period, an enhanced peak current response with no shift in peak potential was observed for the addition of 50 μM hydrazine. Additionally, the acceptable storage stability of *f*-MWCNTs/pTBO/GCE was evident from the final peak current response 2.45 % of initial response current (*I_p*).

The repeatability and reproducibility studies for *f*-MWCNTs/pTBO/GCE were conducted in the presence of 50 μM hydrazine. The fixed value of scan rate was 50 mV/s. Six uninterrupted measurements were performed with single fabricated electrode and the RSD (relative standard deviation) value was found to be 2.63 %. It indicates the appreciable repeatability nature of our modified electrode. In order to determine the reproducibility behavior of our sensor, six distinct measurements were carried out using six individual modified electrodes. The evaluated value of RSD (2.13%) reveals the considerable reproducibility of *f*-MWCNTs/pTBO modified GCE.

3.7 Determination of hydrazine in real samples

The feasible practicality of our modified fabricated electrode was demonstrated in rain, tap and tap water samples. The spiked concentrations (50 μM and 100 μM) of hydrazine in the water samples were determined using amperometric *i-t* technique (**Table 2**). The obtained recovery results were quite satisfactory and support the better practicability of *f*-MWCNTs/pTBO/GCE in real time analysis.

Table 2. Determination of hydrazine in various rain, tap and lake water samples at *f*-MWCNTs/pTBO/GCE

Samples	Added (μM)	Found (μM)	Recovery (%)	RSD* (%)
Rain water	50	50.9	101.8	3.6
	100	99.3	101.6	3.3
Tap water	50	49.5	96.8	4.2
	100	100.2	101.2	3.1
Lake water	50	48.9	102.2	3.6
	100	100.6	101.4	2.9

4. CONCLUSIONS

To conclude, *f*-MWCNTs/pTBO based hydrazine sensor has been constructed through facile electrochemical approach. Relative to previously reported hydrazine sensors, low overpotential and good electrocatalytic activity were exposed by our fabricated electrode. The electroanalytical parameters namely, linear range, LOD and sensitivity were evaluated to be 1–357 μM , 0.24 μM and 2492 $\mu\text{A mM}^{-1} \text{cm}^{-2}$. The performance of *f*-MWCNTs/pTBO/GCE based on the above mentioned electroanalytical parameters were concordant with the earlier reported sensors for the determination of hydrazine. The selectivity studies expose the appreciable selectivity of our sensors towards hydrazine in presence of other interfering agents with excess concentration. The demonstrated practicability paves the way for our fabricated electrode in future applications such as biosensors, electronics and optics.

ACKNOWLEDGEMENT

This project was supported by the Ministry of Science and Technology and the Ministry of Education of Taiwan (Republic of China). Dr. Rajkumar Devasenathipathy gratefully acknowledges the National Taipei University of Technology, Taiwan for the postdoctoral fellowship.

References

1. J.E. Troyan, Properties, production, and uses of hydrazine, *Ind. Eng. Chem. Res.*, 45 (1953) 2608-2612.
2. Y. Wang, Y. Wan and D. Zhang, *Electrochem. Commun.*, 12 (2010) 187-190.
3. G. Choudhary and H. Hansen, *Chemosphere*, 37 (1998) 801-843.
4. A.R. Zarei, *Anal. Biochem.*, 369 (2007) 161-167.
5. J.W. Mo, B. Ogorevc, X. Zhang and B. Pihlar, *Electroanalysis*, 12 (2000) 48-54.
6. J.S. Budkuley, *Microchimica Acta*, 108 (1992) 103-105.
7. S.W. Thomas and T.M. Swager, *Adv. Mater.*, 18 (2006) 1047-1050.
8. A. Safavi and M. Baezzat, *Anal. Chim. Acta.*, 358 (1998) 121-125.
9. H. Kirchherr, *J. Chromatogr. B.*, 617 (1993) 157-162.
10. P. Ortega-Barrales, A. Molina-Díaz, M. Pascual-Reguera and L. Capitán-Vallvey, *Anal. Chim. Acta.*, 353 (1997) 115-122.
11. R. Devasenathipathy, V. Mani and S.-M. Chen, *Talanta*, 124 (2014) 43-51.

12. S.K. Kim, Y.N. Jeong, M.S. Ahmed, J.-M. You, H.C. Choi and S. Jeon, *Sens. Actuators, B.*, 153 (2011) 246-251.
13. Z. Meng, B. Liu and M. Li, *Int. J. Electrochem. Sci.*, 12 (2017) 10269-10278.
14. M.-F. Wang, W. Li, P.-J. Hu, S.-S. He, H.-M. Yang and X.-Z. Li, *Int. J. Electrochem. Sci.*, 11 (2016) 1928-1937.
15. H.M. Nassef, A.-E. Radi and C.K. O'Sullivan, *J. Electroanal. Chem.*, 592 (2006) 139-146.
16. M. Mazloum-Ardakani and A. Khoshroo, *Electrochimica Acta*, 103 (2013) 77-84.
17. Y. Umasankar, T.-Y. Huang and S.-M. Chen, *Anal. Biochem.*, 408 (2011) 297-303.
18. Q. Yi, F. Niu and W. Yu, *Thin Solid Films*, 519 (2011) 3155-3161.
19. A.P. Periasamy, Y. Umasankar and S.-M. Chen, *Talanta*, 83 (2011) 930-936.
20. D. Zhang, K. Zhang, Y.L. Yao, X.H. Xia and H.Y. Chen, *Langmuir*, 20 (2004) 7303-7307.
21. J. Zeng, W. Wei, L. Wu, X. Liu, K. Liu and Y. Li, *J. Electroanal. Chem.*, 595 (2006) 152-160.
22. Y. Liu, J. Lei and H. Ju, *Talanta*, 74 (2008) 965-970.
23. V. Rajendran, E. Csöregi, Y. Okamoto and L. Gorton, *Anal. Chim. Acta.*, 373 (1998) 241-251.
24. H. Chang, X. Wang, K.-K. Shiu, Y. Zhu, J. Wang, Q. Li, B. Chen and H. Jiang, *Biosens. Bioelectron.*, 41 (2013) 789-794.
25. S. Vardharajula, S.Z. Ali, P.M. Tiwari, E. Eroğlu, K. Vig, V.A. Dennis and S.R. Singh, *Int. J. Nanomed.*, 7 (2012) 5361.
26. Q. Zhang, J.Q. Huang, W.Z. Qian, Y.Y. Zhang and F. Wei, *Small*, 9 (2013) 1237-1265.
27. G. Vuković, A. Marinković, M. Obradović, V. Radmilović, M. Čolić, R. Aleksić and P.S. Uskoković, *Appl. Surf. Sci.*, 255 (2009) 8067-8075.
28. L. Zheng and J.-f. Song, *Talanta*, 79 (2009) 319-326.
29. R. Sivasubramanian and M. Sangaranarayanan, *Sens. Actuators, B.*, 213 (2015) 92-101.
30. J. Zhao, J. Liu, S. Tricard, L. Wang, Y. Liang, L. Cao, J. Fang and W. Shen, *Electrochimica Acta*, 171 (2015) 121-127.
31. S. Kaviani, S.N. Azizi and S. Ghasemi, *J. Mol. Liq.*, 218 (2016) 663-669.
32. L. Zheng and J.-f. Song, *Sens. Actuators, B.*, 135 (2009) 650-655.
33. M.M. Ardakani, P. Rahimi, H.R. Zare and H. Naeimi, *Electrochimica Acta*, 52 (2007) 6118-6124.
34. M. Mazloum-Ardakani, Z. Taleat, H. Beitollahi and H. Naeimi, *Nanoscale*, 3 (2011) 1683-1689.
35. M. Revenga-Parra, E. Lorenzo and F. Pariente, *Sens. Actuators, B.*, 107 (2005) 678-687.
36. Yuhua Dong, Ziyin Yang, Qinglin Sheng and Jianbin Zheng, *Colloids Surf., A*, 538 (2018) 371-377.
37. Yuxin Zhanga, Binbin Huanga, Jiaping Yeb and Jianshan Ye, *J. Electroanal. Chem.*, 801 (2017) 215-223.